Journal of Colloid and Interface Science 362 (2011) 567–574

Contents lists available at ScienceDirect

Journal of Colloid and Interface Science

www.elsevier.com/locate/jcis

High-speed droplet actuation on single-plate electrode arrays

Arghya Narayan Banerjee [a], Shizhi Qian [a,b], Sang Woo Joo [a,*]

[a] School of Mechanical Engineering, Yeungnam University, Gyeongsan 712-749, South Korea
[b] Institute of Micro/Nanotechnology, Old Dominion University, Norfolk, VA 23529, USA

ARTICLE INFO

Article history:
Received 24 May 2011
Accepted 6 July 2011
Available online 18 July 2011

Keywords:
Co-planar electrode
Electrowetting-on-dielectric
Droplet
Microfluidics

ABSTRACT

This paper reports a droplet-based microfluidic device composed of patterned co-planar electrodes in an all-in-a-single-plate arrangement and coated with dielectric layers for electrowetting-on-dielectric (EWOD) actuation of discrete droplets. The co-planar arrangement is preferred over conventional two-plate electrowetting devices because it provides simpler manufacturing process, reduced viscous drag, and easier liquid-handling procedures. These advantages lead to more versatile and efficient microfluidic devices capable of generating higher droplet speed and can incorporate various other droplet manipulation functions into the system for biological, sensing, and other microfluidic applications. We have designed, fabricated, and tested the devices using an insulating layer with materials having relatively high dielectric constant (SiO_2) and compared the results with polymer coatings (Cytop) with low dielectric constant. Results show that the device with high dielectric layer generates more reproducible droplet transfer over a longer distance with a 25% reduction in the actuation voltage with respect to the polymer coatings, leading to more energy efficient microfluidic applications. We can generate droplet speeds as high as 26 cm/s using materials with high dielectric constant such as SiO_2.

1. Introduction

Droplet-based microfluidics is an emerging technology that involves manipulation of discrete fluid micropackets of controlled volume and composition. It has a wide range of applications in micro-total analysis system (μ-TAS) for biochemical reactions, detections, and other fluidic functions such as microelectronic cooling [1–6]. Generally, microdroplet manipulation can be performed either inside a microchannel [7,8] or in a non-channel configuration [1–4]. Closed channel manipulation of microdroplet is similar to the standard continuous flow microfluidic techniques, but non-channel configuration offers several advantages over the closed channel system, including simpler configuration, two-dimensional movement of the droplets that increases the degrees of freedom of fluid motion, increase in flexibility by electrically driven operation with the introduction of floating electrode system, and elimination of external pressure sources, thus avoiding the need for adding related accessories, such as pumps and valves.

The droplet manipulation has been performed by various driving mechanisms, such as thermocapillary effect [9], surface acoustic wave pumping [10], pressure gradient [11], thermopneumatic pressure gradient [12], surfactant-controlled electrochemical methods [13], asymmetrical surface structuring [14], photochemical effects [15], dielectrophoretic methods [16,17], electrostatic actuation [18], continuous electrowetting [19], electrowetting [1,2,20], and electrowetting-on-dielectric (EWOD) [20]. Amongst these techniques, the surface tension modulation at the solid–liquid interface is very popular because of the site-specific control and localization of surface forces at microscale, which leads to more flexible, scalable, and simpler systems to design and operate. Specifically, the modulation of surface tension via voltage-driven mechanism is more attractive mainly because of the lesser power consumption and heat dissipation. And, particularly, the EWOD technique, which uses the modification of wettability of liquid droplets on a solid insulating surface via electric potential, is very much promising due to the chemical inertness of the surface and possibility of using polarizable and (or) conductive liquids [21]. Several groups are extensively working on the EWOD-based actuation of liquid droplets for biomedical applications in μ-TAS [1–6,20–27]. These groups mainly focused on the microfluidic-based instrumentation including 'lab-on-a-chip' systems that essentially depend on control of fluid motion and extensively studied the transportation, merging, separating, and generating liquid droplets in silicone-oil environment. Very few groups studied the manipulation of liquid droplets in air environment, because EWOD in air is much more challenging due to lower contact angle and higher contact angle hystereses than immiscible liquids [6].

Here, we report the on-chip actuation of water droplets in an air-filled environment. We have designed a test device of co-planar electrodes with various dielectric layers to actuate water droplets with considerably high speeds, and their corresponding velocity

* Corresponding author. Fax: +82 53 810 2062.
E-mail address: swjoo@yu.ac.kr (S.W. Joo).

0021-9797/$ - see front matter © 2011 Published by Elsevier Inc.
doi:10.1016/j.jcis.2011.07.014

data, as a function of actuation voltage, are presented. Another goal is to reduce the driving voltage of the EWOD actuation, which is necessary to develop reliable and highly efficient microfluidic systems. Previously, Moon et al. [28] reported the low-voltage actuation of liquid droplets by using small thickness and highly dielectric materials. Basically, this group used a high-dielectric-constant material coated with fluoropolymer in a conventional parallel-plate system (unlike ours, which is a co-planar system) to show a high contact angle modulation in air and discussed on the basic theory involved. Although they have reported some experimental results on the droplet actuation, no data related to the droplet velocity are furnished. Typically, much higher voltage is required to change the wettability of a droplet on a dielectric layer compared with a conductive layer. The required voltage can be reduced either by decreasing the dielectric layer thickness or by increasing the dielectric constant of the layer, thus increasing the capacitance of the insulating layer. But extremely thin layer can produce imperfections within the film that deteriorates the device performance. Therefore, more emphasis should be given on the materials having high dielectric constants.

Also, particular attention is given to the co-planar EWOD system, where a top ground electrode is not used (like traditional two-electrode EWOD system). Instead, an array of electrodes is fabricated in-plane, embedded within the dielectric layer, and one electrode is activated at a time while others are grounded to drive the droplet. This co-planar microfluidic system has recently garnered some interest mainly because of several advantages it offers over the traditional two-plate EWOD systems, such as increased flexibility in liquid dispensing and handling processes due to the absence of top ground plate, simpler packaging process, removal of contact from top plate – thus allowing flexible droplet motion with higher degrees of freedom, easy incorporation (from top) of other droplet actuation techniques such as dielectrophoresis, surface acoustic wave pumping into the system, comfortable use of various laser-based surface analytical and interferometric methods, reduction in viscous drag forces at liquid–solid interface between the droplet and the top cover plate, etc. [1,22,29]. Due to these advantages, several groups in the recent past have reported the use of co-planar electrodes without a top grounded (cover) plate for liquid droplet manipulation [1,16,18,22,29–31].

2. Theoretical analysis

Physically, in the EWOD mechanism, a polarizable liquid droplet, sandwiched between two hydrophobic insulated electrodes, is subjected to a potential difference across the electrodes. Depending on the applied voltage, the wettability of the liquid surface in proximity with the electrodes under higher potential is changed due to the switching of that solid surface from hydrophobic to hydrophilic nature. The relationship between the applied voltage and the changes in the contact angle can be determined using the solid surface dielectric property (average surface charge density) and hydrophobicity and can be expressed by Young–Lippmann equation as [21]

$$\cos\theta^V - \cos\theta^0 = \frac{\varepsilon_r\varepsilon_0}{2\gamma_{LG}d}V^2 = \frac{1}{2\gamma_{LG}}C^AV^2, \tag{1}$$

where θ^0 and θ^V are initial and final (under applied voltage, V) contact angles, respectively, ε_r is the relative permittivity, ε_0 is the permittivity of vacuum, γ_{LG} is the liquid–gas interfacial energy (surface tension), d is the dielectric layer thickness, and C^A is the capacitance per unit area of the active electrode. The above equation clearly shows that the change in the contact angle can be modified by manipulating either the applied voltage or the properties of dielectric layer (or both). Also for certain (pre-determined) change in the contact angle, the applied voltage can also be minimized accordingly.

For driving the liquid droplet over an array of co-planar electrodes using EWOD actuation process, the liquid droplet is initially resting on two co-planar embedded electrodes, one of which is active and the other is not, whereas the droplet is grounded from the top (as shown in Fig. 1) with a hydrophobized cover plate. Due to the voltage difference between the active and grounded electrodes, the contact angle of one side of the droplet in contact with the active electrode will change with respect to that of the inactive one, creating a pressure difference between the right and left menisci of the droplet, which can be expressed as [20]

$$\Delta p = \frac{\gamma_{LG}}{t}(\cos\theta^V - \cos\theta^0) = \frac{1}{2t}c^AV^2 = \frac{\varepsilon_r\varepsilon_0}{2td}V^2, \tag{2}$$

where t is the distance between the co-planar electrodes and the cover grounded plate in a parallel-plate arrangement. Due to this pressure difference, the droplet will move forward, as indicated in the figure. By sequentially actuating the embedded electrodes, one can move the droplet accordingly, provided that the leading meniscus of the droplet always touches one of the active electrodes while the receding one touches the inactive one.

As far as the droplet actuation via co-planar arrangement of electrode system (without using top grounded plate) is concerned, Yi and Kim [29] demonstrated the droplet actuation through all-in-a-single-plane electrode arrangement without using the cover plate with various microfluidic operations on the test device. Also, they have mathematically calculated the driving pressure difference (Δp) across the liquid droplet for actuation on co-planar electrodes with an electrode-free (floating) cover plate, which can be expressed as [29,32]

$$\Delta p = \frac{\varepsilon_r\varepsilon_0}{2td}\left[\frac{A^A}{A^{Tot}}\left(\frac{A^{Gr}}{A^A+A^{Gr}}\right)^2 + \frac{A^{Gr}}{A^{Tot}}\left(\frac{A^A}{A^A+A^{Gr}}\right)^2\right]V^2, \tag{3}$$

where A^A and A^{Gr} are the areas over the active (driving) electrode and ground electrode, respectively, and $A^{Tot} = A^A + A^{Gr} + A^{Gap}$ (A^{Gap} = area over the electrode gap). Eq. (3) depicts that the driving pressure is dependent on the area ratios of active and grounded electrodes as well as the gap between them. Δp will be optimized for A^A and A^{Gr} to be equal and for A^{Gap} to be minimum [24]. The shapes of the droplets in a co-planar arrangement of electrodes with and without the use of electrode-free cover plate are shown in Fig. 2a and b, respectively. When the droplet is actuated via co-planar arrangement of electrode system without using any cover

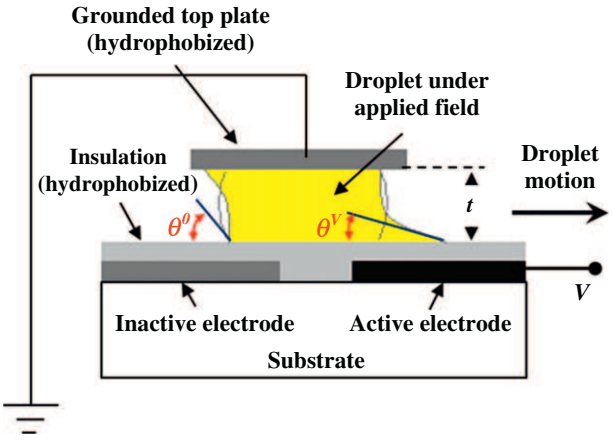

Fig. 1. Schematic description of EWOD actuation of a liquid droplet by conventional parallel-plate system where the droplet is sandwiched between co-planar electrodes arrays and top grounded electrode (figure is not to the scale). The contact angle (θ^0) without any applied voltage changes to θ^V when the active electrode is subjected to an applied voltage V.

plate (cf. Fig. 2b), the expression for pressure difference will be mathematically more complicated because the internal pressure variation within the droplet will be non-uniform. The corresponding equivalent device circuit is schematically shown in Fig. 2c. The capacitances of dielectric layers over the driving (active) electrode, C^A, and that of the grounded electrode, C^{Gr}, and the area of the inter-electrode gap will determine the driving force required for droplet actuation [33]. But, in any case, the expression for pressure difference will be similar to Eq. (3), which involves the areas of active and grounded electrodes as well as the gap between them. It can be optimized by using the area ratio between the active and the grounded electrodes as unity and keeping the gap-area between the electrodes to a minimum value within the experimental limit.

In this present work, the reported device is designed to consist of patterned electrodes on glass substrate coated with dielectric layer for EWOD actuation of discrete droplets. The embedded co-planar electrodes are fabricated with identical areas, so that the area ratio between the active and grounded electrodes becomes unity. Also, the gap between the active and grounded electrodes is minimized to less than 3% with respect to that of active electrodes, within our experimental limit to optimize the driving pressure. One of the goals of the device fabrication is to reduce the actuation voltage of the droplets for reliable microfluidic systems. We have thus used materials with relatively high dielectric constant such as silicon dioxide and compared the results with low dielectric constant polymer coatings (e.g., Cytop). Also, we aimed to increase the droplet speed along the patterned electrodes, which is a necessary step for realization of high-efficient droplet-based microfluidic devices. In most of the previous works based on single-plate co-planar electrode arrays [18,22,25,28,29,33,34], the droplet velocity is found to be very low (10–16 mm/s) [24,28]. Also, most of these works are based on theoretical calculation of energy distribution and pressure difference of the droplet for improved droplet translation [22,29,33]. Although one group reported the theoretical estimation of droplet velocity in co-planar system against parallel one, no experimental data have been presented [34]. We have presented experimental data on the droplet velocity with respect to actuation voltage to show considerably high speed of the droplet against the reported values and show that the data fit well with the existing theory. The co-planar EWOD test device reported here would provide necessary flexibility to the existing microfluidic systems for the realization of multilayer EWOD structures with multiple sensing and driving mechanisms and improved capacities for wide range of microfluidic applications.

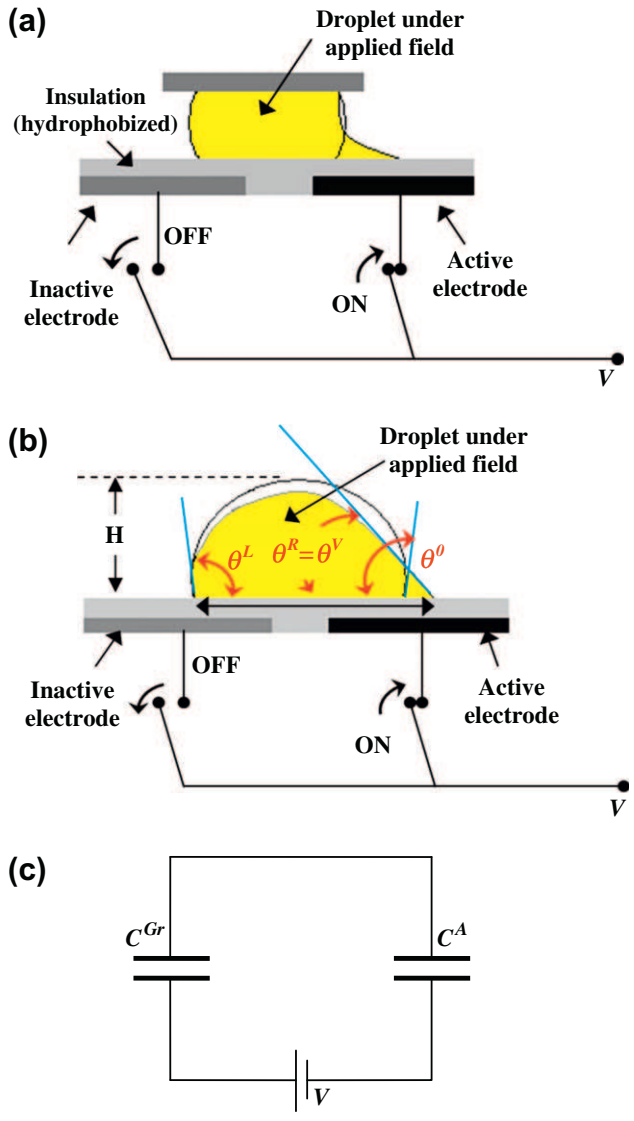

Fig. 2. Schematic descriptions of the shapes of the droplet with and without the external field for (a) top ungrounded cover plate (b) without a top cover plate. Under an applied voltage (V) to the right electrode (active), the contact angle changes from θ^0 to θ^V ($=\theta^R$). H is the reduced height of the droplet under the applied field (figures are not to the scale). (c) Equivalent circuit diagram for Fig. 2(b). C^A is the capacitance of the dielectric layer over the driving (active) electrode, and C^{Gr} is the same for grounded (inactive) electrode.

3. Experimental

The proposed device is shown in Fig. 3a. It consists of a glass substrate, on which metal electrodes are patterned photolithographically, followed by dielectric and hydrophobic layer deposition. The device is fabricated by standard microfabrication techniques. Substrate cleaning is done by standard procedure using isopropyl alcohol, acetone, and piranha stripper. For photolithography materials, standard negative photoresist (AL-217, Negative Photoresist kit consisting Negative Photoresist I # 651796, Aldrich, Korea), developer (Negative Resist Developer I # 651788, Aldrich, Korea), photomask, etc. are used. Metallization of driving electrodes is done by a two-target (dual-head) turbo-pumped sputter-coating system (Model # K575XD, Quorum Technologies, UK). Three layers of Cr (25 nm)/Au (50 nm)/Cr (25 nm) metals are used (cf. Fig. 3). Cr is used as the buffer layer between the Au pads and the glass substrate mainly because of the migration of oxygen from the substrate to the initial Cr layer during nucleation stage of Cr deposition, which enables the efficient sticking of the metal coatings. For similar reasons, Cr is also used as the intermediate layer between the gold electrodes and SiO_2 dielectric layer. Schematic diagram of the photolithography steps is shown in Fig. 3b. Initially, photoresist is spin-coated (Midas System, Model # SPIN-1200D) on glass substrates (FisherScientific, Korea), followed by mask exposure, patterning, and development. Thereafter, electrode patterns are created via sputtering technique and removal of photoresist to obtain the final electrode arrays. Before creating the electrodes, the patterned substrates are dry-cleaned by a plasma cleaner (Femto Science) for proper sticking of the metals on the substrates. Next, standard radiofrequency (r.f.) sputtering technique (Emitech Co. Ltd.) is used to deposit 300 nm SiO_2 layer on top of the electrodes. Finally, Cytop (AiTheR Corp., Korea/AGC Chemicals, Japan) is deposited as a hydrophobic layer. Two-step spin coating technique is used (@ 2000 rpm for 30 s each followed by baking @ 85 °C and annealing @ 180 °C) to deposit 2 μm Cytop layer on top of SiO_2 layer. To get the final electrode pattern on the substrate, selective wet-etching is carried out using gold and Cr etchants (Duskan Pure Chemicals, Korea).

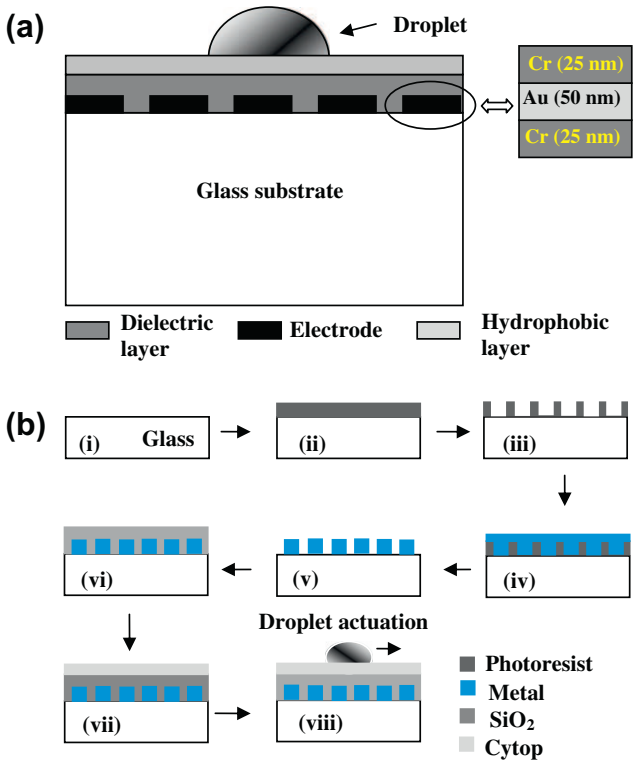

Fig. 3. (a) Schematic cross-sectional view of the test structure of a droplet actuation device. Inset shows the magnified view of the actual structure of each electrode. (b) Schematics of the various photolithographic steps for the fabrication of the device: (i)/(ii) glass substrate spin-coated with photoresist, (iii) pattern transfer, (iv)/(v) metal electrode array formation, (vi)/(vii) dielectric/hydrophobic layer(s) deposition and (viii) droplet actuation (the structure is not to the scale).

It must be mentioned here that in another variation of the experiments, we have used only 2 μm Cytop as both dielectric as well as hydrophobic layer to see its effect on the droplet actuation. This is mainly done to observe the effect of dielectric properties of these two types of insulators on droplet actuation. We have fabricated two types of device structures, one with SiO_2 as the dielectric layer and the other with Cytop as the dielectric material. From here on, we will mention the former one as 'SiO_2-dielectric device' and the latter as 'Cytop-dielectric device'. The fabricated lab-on-a-chip device is then packaged by standard thermosonic gold wire bonding technique (Kulicke and Soffa) for actuation of liquid droplets. Standard relay system (Keithley) with a dc power supply (Thermo-Scientific) is used for droplet actuation using a GPIB interface through LabView software. The motion of the liquid droplet is recorded by a high-speed camera (Redlake, MotionXtra N4) with the Motion Studio camera control software. The droplets are dispensed on the device by a standard syringe, and the volume is kept constant (within the experimental limit) for all the droplet transfer experiments, which is around 3.0 μL. The error in the volume of the dispensed liquid droplet is measured to be less than 5%. The liquid droplets are actuated at different voltages ranging from 80 V to 200 V. Twelve electrodes with 0.5 mm × 2.0 mm (width × length) dimension and 15-μm electrode spacing have been actuated sequentially by a control system with the electrode ON time ranging from 10 ms to 2 ms and OFF time around 500 μs.

To calculate the operating ranges of voltages for SiO_2-dielectric and Cytop-dielectric devices before dielectric breakdown, we have considered $V_{optimum}$ as the maximum voltage required for a dielectric layer of certain thickness d before breakdown and related to the breakdown field ($E_{breakdown}$) as

$$V_{optimum} = V_{breakdown} = dE_{breakdown}. \quad (4)$$

It is well known that the breakdown field for sputter-deposited SiO_2 layer (as in our case) is around 10 MV per cm of thickness [35], whereas for Cytop layer, this value is around 1 MV per cm of thickness at room temperature [36]. Using these values, the maximum allowable voltage before dielectric breakdown becomes around 300 V for SiO_2 layer and around 200 V for Cytop layer. Therefore, we have designed and operated our devices within these voltage limits to make sure that no electrolysis is taking place within our microdroplets due to dielectric breakdown.

4. Results and discussion

Fig. 4 shows four video frame images of a moving droplet at 2-ms interval (frame rate ~1000 fps with a resolution of 1280 × 1024). The required actuation voltage is around 110 V, with an electrode ON time of 2 ms. White lines are drawn to the leading meniscus of the droplet to indicate the movement. Red arrows indicate the direction of the motion. In the top-most frame, 110 V is applied at the

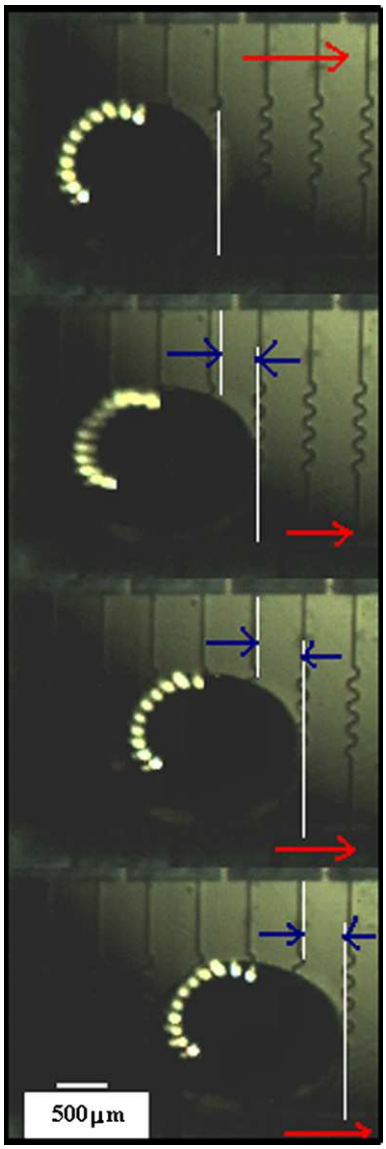

Fig. 4. Video frame images of moving droplet at 2-ms intervals. White lines represent the leading meniscus of the moving droplet, and red line represents the direction of the motion. Blue arrows are drawn to show an estimate of the droplet displacement with respect to the electrode arrays. Black zigzag lines are the electrode gaps (15 μm). (For interpretation of the references to color in this figure legend, the reader is referred to the web version of this article.)

electrode underneath the droplet's leading meniscus while the adjacent electrodes are grounded. In the subsequent frames, the 110 V potential is switched to the adjacent electrodes along the direction shown by the arrows and the droplet follows. The white dots in the figure are actually the reflection of the illuminating light of the microscope into the water droplet. Fig. 5a represents the velocity–time (V–t) graph of the microdroplet at various actuation voltages ranging from 90 V to 110 V, with 2 ms electrode ON time for all cases. The device structure in this case consists of SiO_2 as the dielectric layer and Cytop as the hydrophobic layer. The velocities and distances covered by the droplets are calculated by the image analyses of the camera software. The resolution for determining the position is 5 μm. The distance covered is measured from the displacements of the droplet in each frame, and the corresponding velocities are determined from the frame rate. Since the droplet is observed to be non-uniformly elongated along the direction of motion, all the displacements are calculated with respect to the leading meniscus of the droplet. Also, it has been observed that the instantaneous displacement and velocity of the droplet is non-uniform, as evidenced by the video analysis of the moving droplet over the course of a single transfer. The trajectory of the droplet is very similar to a staircase motion reported by Cooney et al. [22], where the droplet motion is centered on the electrode gap between an activated and a grounded electrode in each actuation step. Therefore, the velocity data are averaged out and plotted against a mean curve over the period of a single droplet transfer. The velocities are observed to increase initially and then attain a steady value with further increase in time. The maximum steady velocity is found to be around 26.0 cm/s for 110 V actuation voltages, which is much higher than the conventional parallel-plate system (~10 cm/s) [1], and comparable to the previously reported value for co-planar system by Kim and co-authors (~24.0 cm/s) [37], where alternating potentials with relatively higher root-mean-square (r.m.s.) values at high frequencies are used. A comparison of various droplet manipulation parameters of our system and previously reported systems is furnished in Table 1. From the table, it is clearly shown that the current system reported here provides very high droplet velocity at a relatively lesser actuation voltage compared with parallel-plate and single-plate systems reported earlier. Most of them either achieved much lesser maximum velocity when operated at a relatively lower voltage or needed much higher actuation voltage to achieve comparable droplet speed with respect to ours. Also considering the as-fabricated electrode configurations and dimensions along with the electrode ON/OFF times mentioned in the experimental section, the calculated maximum velocities are coming out around 20–25 cm/s and hence tallies well with the experimental values. As mentioned earlier, in another variation of the experiment, we have used only 2 μm Cytop as both dielectric and hydrophobic layer to see its effect on the droplet actuation. Fig. 5b represents the V–t plots for Cytop-dielectric devices with actuation voltages vary from 100 V to 150 V, with 3 ms electrode ON time. Here also the velocities are found to increase slowly and then attain a steady velocity with further increase in time. Maximum steady velocity obtained in a consistent manner is around 15.0 cm/s for 150 V actuation voltages.

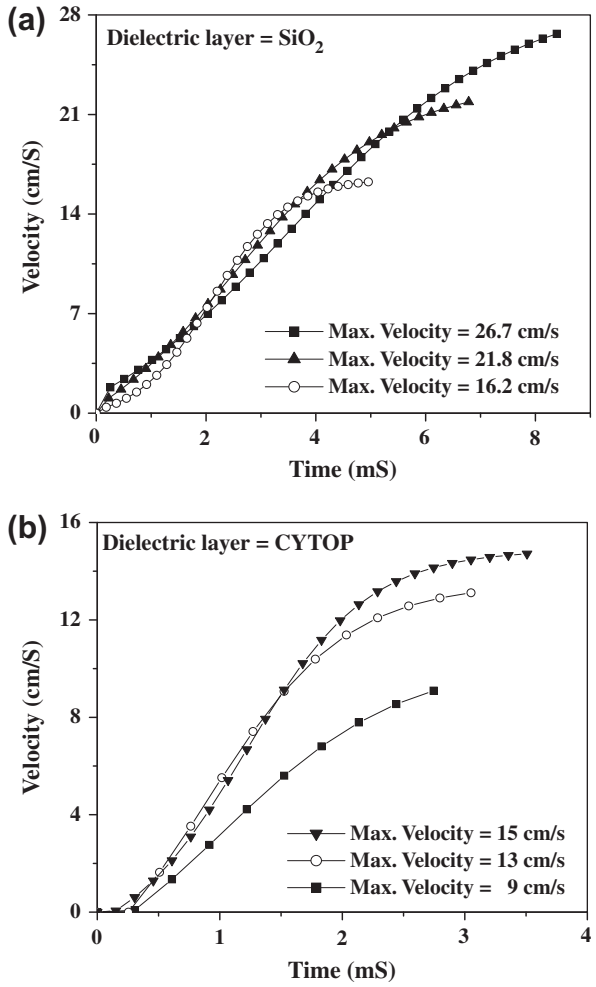

Fig. 5. Temporal variations of droplet velocity for (a) SiO_2-dielectric devices at different actuation voltages of (■) 110 V, (▲) 100 V and (○) 90 V, (b) Cytop-dielectric device for different actuation voltages of (▲) 150 V, (○) 120 V and (■) 100 V.

Also, it must be mentioned in this connection that all the velocity graphs are plotted up to the steady-state motion of the droplet. Previously, Pollack et al. [1] reported the temporal variation of velocity and displacement of a 0.1 M KCl droplet in a conventional two-plate EWOD electrodes system and obtained a maximum droplet velocity around 10 cm/s using a DC voltage pulse across a series of four adjacent electrodes at a fixed switching rate. They have also observed similar nature of the V–t curves, as obtained by us, where the droplet velocity increases slowly to an optimum value and then decelerates to zero velocity. In our case, we have also observed the increase in the velocity to an optimum value and then to a steady velocity before decelerating to rest. We aimed to transfer the droplet with a steady velocity over a certain distance, and thereafter, the droplet decelerates at the end of the transfer. But in the graphs, we have only shown the attainment of the steady velocity of the droplet, which clearly shows that the droplet can be transferred steadily over a considerable distance if the device is designed accordingly with proper sequential voltage switching process across the electrodes. The deceleration portion is not shown for clarity. To estimate the moving distance of the droplet during a single transfer, we have plotted the temporal variation of the displacement of the droplet during one operation (cf. Fig. 6). The device in this case is taken as the SiO_2-dielectric device, whereas the actuation voltage is kept at 110 V to get highest droplet velocity as determined from Fig. 5a. It has been observed that, under the above-mentioned conditions, on an average, a droplet can be transferred up to 8 electrodes (equivalent to 0.4 cm linear distance) in a consistent manner. Beyond that the droplet starts lagging behind the voltage actuation rate. We believe that, instead of a constant voltage switching rate, a variable switching rate (higher in the acceleration portion and lesser in the steady-state portion) of the voltage actuation can improve the droplet transfer over a longer distance. Preliminary study proves to support this idea, but better optimization of the conditions is needed, which is the further course of our work.

Table 1
Comparison of various droplet actuation parameters of previously reported parallel-plate and single-plate systems with respect to the current system under study.

Device structure	Dielectric layer thickness (μm)	Actuation voltage (V)	Max droplet speed (cm/s)	Environment	Ref.	Remarks
PCB (substrate)/co-planer electrodes/parylene-C (dielectric)/water droplet/grounded top-plate (parallel-plate system)	1.2	110 V (1 kHz AC)	0.5	Air	[38]	Teflon–AF is used as hydro-phobic layer
PCB (substrate)/co-planer electrodes/parylene-C (dielectric)/water droplet/grounded top-plate (parallel-plate system)	0.8	70 V (1 kHz AC)	0.45	Oil	[38]	Teflon–AF is used as hydro-phobic layer
Glass (substrate)/co-planer electrodes/parylene-C (dielectric)/water droplet/grounded top-plate (parallel-plate system)	0.5	80 V (1 kHz AC)	0.45	Air	[38]	Teflon–AF is used as hydro-phobic layer
Glass (substrate)/co-planer electrodes/parylene-C (dielectric)/0.1 M KCl droplet/grounded top-plate (parallel-plate system)	0.8	60 V DC	10.0	Oil	[1]	Teflon–AF is used as hydro-phobic layer
Glass (substrate)/co-planer electrodes/SiO_2 (dielectric)/water droplet/grounded top-plate (parallel-plate system)	0.1	150 V (1 kHz AC)	24.0	Air	[37]	Teflon–AF is used as hydro-phobic layer
Glass (substrate)/co-planer electrodes/SU-8 (dielectric)/water droplet (single-plate system)	1.0	90 V (9 Hz square wave)	2.4	Air	[39]	Teflon–AF is used as hydro-phobic layer
Glass (substrate)/co-planer electrodes/SiO_2 (dielectric)/water droplet/cover plate (parallel-plate system, but top-plate ungrounded)	0.3	65 V (1 kHz AC)	0.45	Air	[29]	Cytop is used as hydro-phobic layer
Glass (substrate)/Co-planer electrodes/SiO_2 (dielectric)/water droplet (single-plate system)	0.3	65 V (1 kHz AC)	1.0	Air	[29]	Cytop is used as hydro-phobic layer
Si (substrate)/co-planer electrodes/Ta_2O_5 (dielectric)/water droplet (single-plate system, with co-planar ground line is used between active and passive electrodes)	0.095	15	1.6	Air	[33]	Teflon–AF is used as hydrophobic layer
Glass (substrate)/co-planer electrodes/SiO_2 (dielectric)/water droplet (single-plate system)	0.3	110 V	26.0	Air	*Current study*	Cytop is used as hydro-phobic layer
Glass (substrate)/co-planer electrodes/Cytop (dielectric)/water droplet (single-plate system)	2.0	150 V	15.0	Air	*Current study*	Cytop is used as hydro-phobic layer

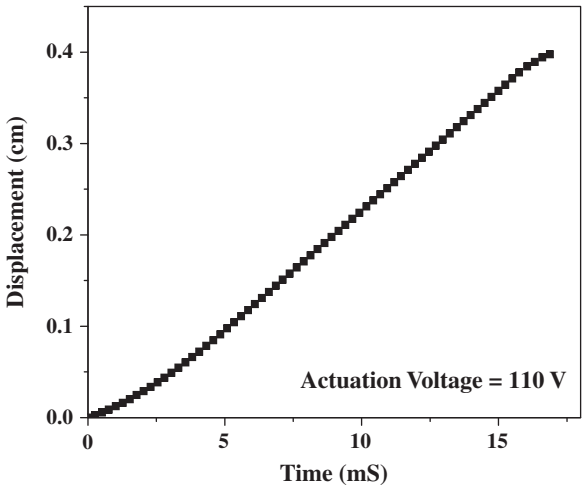

Fig. 6. Temporal variation of droplet displacement over a single transfer for SiO_2-dielectric device at an actuation voltage of 110 V.

Physically, the driving pressure for droplet actuation, as expressed in Eqs. (2) and (3), is maximum when the potential difference between the active and inactive (grounded) electrodes is maximum, in which case the inactive electrode is assumed to be perfectly grounded. But in practical cases, due to the finite value of discharging time, the potential difference between the active and adjacent 'grounded' electrodes is smaller than the maximum value, which produces weaker driving force for droplet actuation. For materials with higher capacitance, the discharging time is shorter, so that the driving pressure is higher, leading to a higher value of droplet velocity. Due to this reason, we have seen that for similar actuation voltages, SiO_2-dielectric devices (dielectric constant = 3.9) generate relatively higher droplet velocities with respect to Cytop-dielectric devices (dielectric constant = 2.1), as depicted in Fig. 5a and b. The results clearly indicate that nearly 25% decrease in the actuation voltage is achieved with materials having high dielectric constant with respect to polymer coatings to get similar droplet motion.

To estimate the droplet velocity, we consider a liquid droplet of volume V sitting on a co-planar EWOD structure with no cover plate (cf. Fig. 2b). The droplet velocity over the single planar device, $U_{single\text{-}plate}$, is estimated by balancing the forces arising from the surface tension (γ_{LG}, between liquid–air interface) and viscous surface-shear stress (Γ) on the droplet, assuming any other contact line frictional or resistive or drag forces to be negligible. The shearing stress (Γ) is estimated based on the peak velocity near two-fifth of the droplet height, H (as used in many numerical calculations), and the corresponding shear force (F_{Shear}) is expressed as [34]

$$F_{\text{Shear}} = \Gamma \pi r^2 = \frac{5\mu U_{single\text{-}plate}}{2H}\pi r^2, \tag{5}$$

where πr^2 is the area covered by the droplet over the electrodes, assuming it to be the projection of a spherical droplet and μ is the viscosity. Similarly, the force related to surface tension (F_{ST}) is expressed as

$$F_{ST} = 2r\gamma_{LG}(\cos\theta^R - \cos\theta^L), \tag{6}$$

where $\theta^R$and θ^L are the contact angles at right and left menisci of the droplet under the applied field. Equating these two forces, the expression for droplet velocity is as

$$U_{single\text{-}plate} = \frac{4H\gamma_{LG}}{5\pi\mu r}\left(\cos\theta^R - \cos\theta^L\right). \quad (7)$$

Considering the maximum droplet velocity as 26.0 cm/s (for SiO_2-dielectric devices at 110 V, cf. Fig. 5a) and assuming the droplet to be hemispherical during actuation and the initial contact angle around 90°, the change in the contact angle ($\Delta\theta$) in the leading meniscus of the droplet becomes approximately 40°, which is indeed in the range of contact angle changes that are used in EWOD devices [1,22,28,29]. Particularly, Moon and co-authors [28] showed a similar 40° change in the contact angle in air for a parallel-plate system, whereas Yi and Kim [29] reported similar changes for co-planar system using similar EWOD materials.

Also to compare the velocity of the droplet on a single planar device ($U_{single\text{-}plate}$) with respect to conventional parallel electrode system, we have calculated the droplet velocity for such parallel electrode system ($U_{parallel\text{-}plate}$) considering a droplet of volume V, and radius r, to be sandwiched between two plates with an electrode gap, t. By similar argument, as furnished above, we have balanced the surface tension force and shearing force, considering the shear stress as $\frac{6\mu U_{parallel\text{-}plate}}{2t}$, based on a planar Poiseuille flow. Hence, the expression for the velocity becomes

$$U_{parallel\text{-}plate} = \frac{\gamma_{LG}t}{6\pi\mu r_{parallel\text{-}plate}}\left(\cos\theta^R - \cos\theta^L\right), \quad (8)$$

where $r_{parallel\text{-}plate}$ is the radius of the droplet in the parallel-plate sandwich structure. Comparing Eq. (7) with Eq. (8), the ratio between the droplet velocities in co-planar and parallel electrode systems is

$$\frac{U_{single\text{-}plate}}{U_{parallel\text{-}plate}} = \frac{24Hr_{parallel\text{-}plate}}{5tr_{single\text{-}plate}}, \quad (9)$$

where $r_{single\text{-}plate}$ is the droplet radius as shown in Fig. 2b for single-plate system. Now if we consider identical volume of liquid droplet for both parallel-plate and co-planar arrangements, then in normal circumstances, we will always get $H \geqslant t$, and $r_{single\text{-}plate} \leqslant r_{parallel\text{-}plate}$, which will lead to $U_{single\text{-}plate} > U_{parallel\text{-}plate}$ [34]. Therefore, assuming equivalent electrowetting properties and parameters in both cases, it can be concluded that the co-planar arrangement of EWOD device without using any top cover plate may provide higher droplet velocity with respect to conventional parallel-plate EWOD system. Indeed, Yi and Kim [29] previously reported more than two-fold increment in the droplet speed in an open plate configuration against parallel-plate system because of the absence of resistance from the top plate, which is consistent with the above discussions.

As far as the evaporation effect of the droplet is concerned, it has been reported earlier that in an open air condition without top cover plate, a 5-μL water droplet generally takes nearly half-an-hour to evaporate from a hydrophobic surface (like Teflon, Cytop, etc.) under laminar flow [22]. Therefore, evaporation rate is expected to decrease in the absence of any convective air flow. Mathematically, evaporation time (τ) of a hemispherical droplet in a non-convective air ambient condition can be represented as [40]

$$\tau = \frac{r^2}{\delta_v}\frac{\rho_L}{\chi_v(1-\Phi)}, \quad (10)$$

where r is radius of the droplet, ρ_L is the droplet density (=10^3 kg m^{-3}, for water), δ_v is the diffusivity of water vapor in air ambient (=26.1×10^{-6} m^2 S^{-1}), χ_v is the saturation value of water vapor (=2.32×10^{-2} kg m^{-3}), Φ is the relative humidity (scaled to 1). For a 3-μL water droplet (roughly 1 mm radius of spherical droplet in our case) in a 0% humid non-convective condition, the evaporation time is coming out around 25–30 min, which is sufficient enough for our droplet transfer experiment as well as for many digital microfluidic applications [22].

5. Conclusions

A design and microfabrication process is presented for high-speed actuation of liquid microdroplets in air-filled environment. The test device consists of the all-in-a-single-plane actuation electrodes without using any top cover or grounded plate. The electrodes are coated with different dielectric layers. The device that is coated with high dielectric material, such as SiO_2, produces significantly high speed of the droplets at a considerably low actuation voltage compared to the low dielectric-coated (polymer) devices. Also it has been observed that the high dielectric material coating provides more efficient and reproducible droplet actuation with a speed as high as 26 cm/s at an actuation voltage of 110 V. Almost 25% reduction in the actuation voltage is obtained for SiO_2-dielectric devices with respect to polymer coatings. Also calculations show that single-plate electrode arrangement of microfluidic system can provide higher velocity with respect to conventional parallel-plate EWOD systems due to the elimination of resistance from the top cover plate. Thus, it can be concluded that this single-plate, co-planar EWOD structure will simplify the device manufacturing process along with easy integration of various liquid-handling and automation processes into the system for potential biological and sensing applications.

Acknowledgment

Financial support of World Class University Grant No. R32-2008-000-20082-0 of the Ministry of Education, Sci. & Technol. of Korea is acknowledged.

References

[1] M. Pollack, A. Shenderov, R. Fair, Lab Chip 2 (2002) 96.
[2] M. Pollack, R. Fair, A. Shenderov, Appl. Phys. Lett. 77 (2000) 1725.
[3] P. Paik, V.K. Pamula, R.B. Fair, Lab Chip 3 (2003) 253.
[4] R.B. Fair, Microfluid. Nanofluid. 3 (2007) 245.
[5] H.C. Orphins, J.C. Nicole, V.G.V. Baret, C. Lasance, M. Baelmans, in: Proc. 2005 IEEE/CPMT 21st Semiconductor Thermal Measurement & Management (SEMI-THERM) Symposium, San Jose, March 15–17, 2005, p. 347.
[6] K.S. Cho, H. Moon, C.J. Kim, J. Microelectrochem. Syst. 12 (2003) 70.
[7] T. Thorsen, R.W. Roberts, F.H. Arnold, S.R. Quake, Phys. Rev. Lett. 86 (2001) 4163.
[8] M. He, J.S. Edgar, G.D.M. Jeffries, R.M. Lorenz, J.P. Shelby, D.T. Chiu, Anal. Chem. 77 (2005) 1539.
[9] T.S. Sammarco, M.A. Burns, AIChE J. 45 (1999) 350.
[10] Z. Guttenberg, H. Muller, H. Habermuller, A. Geisbauer, J. Pipper, J. Felbel, M. Kielpinsky, J. Scriba, A. Wixforth, Lab Chip 5 (2005) 308.
[11] K. Hosokawa, T. Fujii, I. Endo, Anal. Chem. 71 (1999) 4781.
[12] K. Handique, D.T. Burke, C.H. Mastrangelo, M.A. Burns, Anal. Chem. 73 (2001) 1831.
[13] B.S. Gallardo, V.K. Gupta, F.D. Eagerton, L.I. Jong, V.S. Craig, R.R. Shah, N.L. Abbott, Science 283 (1999) 57.
[14] O. Sandre, L.G. Talini, A. Ajdari, J. Prost, P. Silberzan, Phys. Rev. E 60 (1999) 2964.
[15] K. Ichimura, S.K. Oh, M. Nakagawa, Science 288 (2000) 1624.
[16] T.B. Jones, M. Gunji, M. Washizu, M.J. Feldman, J. Appl. Phys. 89 (2001) 1441.
[17] J.A. Schwartz, J.V. Vykoukal, P.R.C. Gascoyne, Lab Chip 4 (2004) 11.
[18] M. Washizu, IEEE Trans. Ind. Appl. 34 (1998) 732.
[19] J. Lee, C.J. Kim, J. Microelectromech. Syst. 9 (2000) 171.
[20] J. Lee, H. Moon, J. Fowler, T. Schoellhammer, C.J. Kim, Sens. Actuators, A 95 (2002) 259.
[21] F. Mugele, J.C. Baret, J. Phys.: Condens. Matter 17 (2005) R705.
[22] C.G. Cooney, C.Y. Chen, M.R. Emerling, A. Nadim, J.D. Sterling, Microfluid. Nanofluid. 2 (2006) 435.
[23] J.S. Hong, S.H. Ko, K.H. Kang, I.S. Kang, Microfluid. Nanofluid. 5 (2008) 263.
[24] K.H. Kang, Langmuir 18 (2002) 10318.
[25] J.K. Park, S.J. Lee, K.H. Kang, Biomicrofluidics 4 (2010) 024102.
[26] S. Berry, J. Kedzierski, B. Abedian, J. Colloid Interface Sci. 303 (2006) 517.
[27] A.I. Drygiannakis, A.G. Papathanasiou, A.G. Boudouvis, J. Colloid Interface Sci. 326 (2008) 451.
[28] H. Moon, S.K. Cho, R.L. Garrel, C.J. Kim, J. Appl. Phys. 92 (2002) 4080.
[29] U.C. Yi, C.J. Kim, J. Micromech. Microeng. 16 (2006) 2053.
[30] A. Torkkeli, A. Haara, J. Saarilahti, H. Harma, T. Soukka, P. Tolonen, in: Proc. 14th IEEE International Conference on Micro Electro Mechanical Systems (MEMS), Interlaken, Switzerland, January 21–25, 2001, p. 475.

[31] F.E. Torres, P. Kuhnt, D.D. Bruyker, A.G. Bell, M.V. Wolkin, E. Peeters, J.R. Williamson, G.B. Anderson, G.P. Schmitz, M.I. Recht, S. Schweizer, L.G. Scott, J.H. Ho, S.A. Elrod, P.G. Schultz, R.A. Lerner, R.H. Bruce, Proc. Natl. Acad. Sci. U.S.A. 101 (2004) 9517.
[32] S. Kwon, L. Lee, in: Tech. Dig. Transducers 2001: 11th International Conference on Solid-State Sensors, Actuators and Microsystems, Munich, Germany, June 2001, p. 1348.
[33] Y. Li, M. Yoshio, L. Haworth, W. Parkes, M. Kubota, A. Walton, in: IEEE Conference on Microelectronic Test Structures, Edinburgh, UK, 2008.
[34] C.Y. Chen, E.F. Fabrizio, A. Nadim, J.D. Sterling, in: Summer Bioengineering Conference, Florida, US, June 25–19, 2003, p. 1241.
[35] S.M. Sze, Physics of Semiconductor Devices, John Wiley and Sons Inc., New York, 1981.
[36] AGC Chemicals (Ahashi Glass Co. Ltd.), Amorphous Fluoropolymer (Cytop) Technical Data Book, October 2004.
[37] S.K. Cho, S.K. Fan, H. Moon, C.J. Kim, in: 15th IEEE International Conference on Micro Electro Mechanical Systems (MEMS), Las Vegas, NV, US, January 20–24, 2002, p. 32.
[38] J. Gong, C.J. Kim, J. Microelectromech. Syst. 17 (2008) 257.
[39] S.K. Fan, H. Yang, T.T. Wang, W. Hsu, Lab Chip 7 (2007) 1330.
[40] H. Hu, R.G. Larson, J. Phys. Chem. B 106 (2002) 1334.